Time-resolved gas-phase kinetic, quantum chemical and RRKM studies of reactions of silylene with alcohols

Rosa Becerra*

Instituto de Quimica-Fisica 'Rocasolano', C.S.I.C., C/ Serrano 119, 28006 Madrid, Spain

J. Pat Cannady

Dow Corning Corporation, P.O. Box 994, Mail CO1232, Midland, Michigan, 48686-0994

Robin Walsh*

Department of Chemistry, University of Reading, Whiteknights, P.O. Box 224, Reading, RG6 6AD, UK

Abstract:

Time-resolved kinetic studies of silylene, SiH_2, generated by laser flash photolysis of 1-silacyclopent-3-ene and phenylsilane, have been carried out to obtain rate constants for its bimolecular reactions with methanol, ethanol, 1-propanol, 1-butanol and 2-methyl-1-butanol. The reactions were studied in the gas phase over the pressure range 1-100 Torr in SF_6 bath gas, at room temperature. In the study with methanol several buffer gases were used. All five reactions showed pressure dependences characteristic of third body assisted association reactions. The rate constant pressure dependences were modelled using RRKM theory, based on E_o values of the association complexes obtained by ab initio calculation (G3 level). Transition state models were adjusted to fit experimental fall-off curves and extrapolated to obtain k^∞ values in the range 1.9 to 4.5 × 10^{-10} cm^3 $molecule^{-1}$ s^{-1}. These numbers, corresponding to the true bimolecular rate constants, indicate efficiencies of between 16 and 67% of the collision rates for these reactions. In the reaction of SiH_2 + MeOH there is a small kinetic component to the rate which is second order in MeOH (at low total pressures). This suggests an additional catalysed

reaction pathway, which is supported by the ab initio calculations. These calculations have been used to define specific MeOH-for-H_2O substitution effects on this catalytic pathway. Where possible our experimental and theoretical results are compared with those of previous studies.

Introduction

Silylene chemistry has been of interest for many years[1]. Silylenes are important reactive intermediates in the photochemical and thermal reactions of organosilicon compounds. Their chemistry has practical significance in industrial applications involving chemical vapour deposition (CVD) leading to formation of electronic device materials. Time-resolved kinetic studies of the simplest silylene, SiH_2, have shown it reacts rapidly with many chemical species at close to collision rates.[2-4] This can be readily understood in terms of its structure. Silylene is a ground state singlet species ($^1A_1$) with an electron pair in a hybrid orbital and a vacant orbital of π symmetry. This empty orbital means that SiH_2 is highly electrophilic and electron donors will readily coordinate to silicon through the vacant orbital to form a silylene-base complex. If the electron donor (Lewis base) is an alcohol, this complex is zwitterionic in nature. Complexes of silylenes with alcohols have been directly observed in low temperature matrices[5] and in solution[6-8]. SiH_2-complexes can, in principle, react further by H-transfer from oxygen to the Si atom[1,3-4,9]

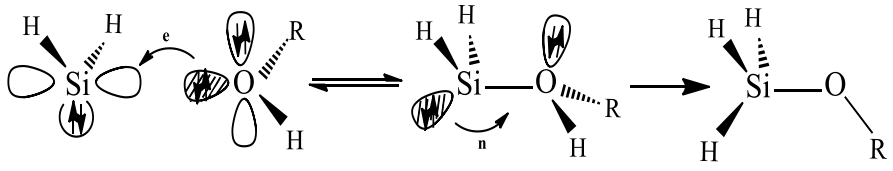

Theoretical calculations indicate[10-15], however, that this second step, the unimolecular conversion of the complex to a siloxane, has a substantial energy barrier and is therefore likely to be slow. Kinetic studies both in the gas phase[4,14-18] and in solution[6-8,19-20] support the formation of these complexes but no evidence has been found for their unimolecular

isomerisation. As to whether a second step in this mechanism can actually occur, the evidence points to a catalysed conversion of the complex to product. This has been found for the prototype reaction of SiH_2 + H_2O in the gas-phase[15] as well as for the reactions of $SiMe_2$ and $SiPh_2$ with MeOH in solution[8], where the reactions of the complexes with MeOH have been found to occur at close to diffusion controlled rates. The catalysed process for the SiH_2 + H_2O reaction is further supported by theoretical calculations[15].

In order to probe this reaction further, and as part of our investigation of the gas-phase reactions of SiH_2, we turn our attention to its reaction with several alcohols, viz. methanol, ethanol, 1-propanol, 1-butanol and 2-dimethyl-1-butanol. The reaction of SiH_2 with methanol has already been studied theoretically[12-13] and experimentally[14]. Alexander, King and Lawrance (AKL)[14] found the gas-phase reaction to be a pressure dependent, third body assisted association process, consistent with the reversible formation of the zwitterionic complex. Our kinetic studies of SiH_2 with H_2O[15,18] and Me_2O[21] are also consistent with the formation of a complex. In the gas-phase the reaction stops at this stage within the experimental time frame (ca 10^{-6} s) and the catalysed process is only observed (for SiH_2 + H_2O) at low pressures when equilibrium with the complex is established slowly. One of the difficulties of the gas phase studies is that the true bimolecular rate constant (for the formation of the zwitterion), ie the pressure-independent value, can only be obtained by extrapolation. Since association processes of reactive molecules of any class tend to become less pressure dependent as the molecular size and complexity of the substrate species increases, we reasoned that kinetic studies of SiH_2 with larger alcohols should get closer to the high pressure limit of this important prototype reaction of silylene with O-donor molecules. As a secondary question we were also interested as to whether any evidence for the catalysed isomerisation of the $H_2Si{\cdot\cdot}O(H)Me$ complex could be obtained.

We therefore decided to reinvestigate the reaction of SiH_2 with methanol at room temperature using several buffer gases, and in addition, to extend this investigation to the higher alcohols. Our study includes both kinetic measurements, RRKM modelling and quantum chemical calculations in order to obtain as full a picture of the process as possible.

Experimental Section

Equipment, Chemicals and Method. SiH_2 was produced by the 193 nm flash photolysis of phenylsilane ($PhSiH_3$) or 1-silacyclopent-3-ene (SCP) using a Coherent Compex 100 exciplex laser. Photolysis pulses (ca 4 cm × 1 cm cross-section) were fired into a variable temperature quartz reaction vessel with demountable windows, at right angles to its main axis. SiH_2 concentrations were monitored in real time by means of a Coherent 699-21 single-mode dye laser pumped by an Innova 90-5 argon ion laser and operating with Rhodamine 6G. The monitoring laser beam was multipassed between 32 and 40 times along the vessel axis, through the reaction zone, to give an effective path length of up to 1.6 m. A portion of the monitoring beam was split off before entering the vessel for reference purposes. The laser wavelength was set by reference to a known coincident transition in the visible spectrum of I_2 vapour and was checked at frequent intervals during the experiments. The monitoring laser was tuned to 17259.50 cm^{-1}, corresponding to a known strong $^{R}Q_{O,J}(5)$ vibration-rotation transition[22] in the SiH_2 absorption band. Light signals $\tilde{A}\,^1B_1(0,2,0) \leftarrow \tilde{X}\,^1A_1(0,0,0)$ were measured by a dual photodiode/differential amplifier combination and signal decays were stored in a transient recorder (Datalab DL910) interfaced to a BBC microcomputer. This was used to average the decays of between 5 and 20 photolysis laser shots (at a repetition rate of 0.5 or 1 Hz). The averaged decay traces were processed by fitting the data to an exponential form using a non-linear least squares package. This analysis provided the values for first-order rate coefficients,

k_{obs}, for removal of SiH_2 in the presence of known partial pressures of substrate gas. Static gas mixtures were used and the optics were cleaned regularly.

Gas mixtures for photolysis were made up, containing between 2.5 and 2.8 mTorr of SCP or 2.5 and 3.6 mTorr of $PhSiH_3$, a few mTorr of ROH (see following) and inert diluent (SF_6) at added pressures of between 0 and 100 Torr. For each series of experiments the pressures of ROH were: 0-2 Torr of CH_3OH (MeOH), 0-230 mTorr of C_2H_5OH (EtOH), 0-100 mTorr 1-C_3H_7OH (1-PrOH), 0-80 mTorr of 1-C_4H_9OH (1-BuOH), 0-53 mTorr of $C_5H_{11}OH$ (2-MBA). Other buffer gases (N_2, Ar and C_3H_8) were used for the experiments with MeOH. Pressures of N_2 varied from 5 to 200 Torr; of Ar from 10 to 100 Torr and of C_3H_8 from 5 to 40 Torr. Pressures were measured by capacitance manometers (MKS, Baratron).

All gases used in this work were frozen at 77 K and pumped free of any vestiges of air prior to use. $PhSiH_3$ (99.9%) was obtained from Ventron-Alfa (Petrarch). SCP was prepared by the reduction of 1,1-dichloro-1-silacyclopent-3-ene with $LiAlH_4$ in ether in 60% yield following literature procedures[23]. SCP was purified by low pressure distillation to greater than 90%. MeOH was from Fisher Scientific (99.9%), EtOH was from BDH (Analar, 99.7-100%), 1-PrOH was from Fisher Scientific (99.8%), 1-BuOH from Acros Organics, (99.4%) and 2MBA from Acros Organics (99%). Sulfur hexafluoride, SF_6, (no GC-detectable impurities) was from Cambrian Gases.

Ab Initio Calculations. The electronic structure calculations were performed initially with the Gaussian 98 and subsequently the Gaussian 03 software packages[24]. All structures were determined by energy minimization at the MP2=Full/6-31G (d) level. Stable structures, corresponding to energy minima, were identified by possessing no negative eigenvalues of the Hessian matrix. The standard Gaussian-3 (G3) compound method[25] was employed to determine final energies for all local minima. For transition states the elements of the G3 method were used, viz: optimization to TS at HF/6-31G(d), frequencies at HF/6-31G(d), optimization to TS at

MP2=full/6-31G(d), followed by four single point energy determinations at the MP2=full/6-31G(d) geometry, viz: QCISD(T)/6-31G(d), MP4/6-31+G(d), MP4/6-31G(2df,p), and MP2=full/G3large, and the values were combined according to the G3 procedure.[25] The identities of the transition state structures were verified by calculation of Intrinsic Reaction Co-ordinates[26] (IRC) at the MP2=Full/6-31G(d) or B3LYP/6-31G(d) levels. Reaction barriers were calculated as differences in G3 enthalpies at 298.15 K. Some free energies values were also obtained.

Results

Kinetics. For each reaction of interest it was independently verified during preliminary experiments that, in a given reaction mixture, k_{obs} values were not dependent on the exciplex laser energy or number of photolysis shots. Because static gas mixtures were used, tests with up to 20 shots were carried out. The constancy of k_{obs} (5 shot averages) showed no effective depletion of reactants in any of the systems. For each system the precursor pressures were kept fixed to ensure a constant (but always small) contribution (k_{int}) to k_{obs} values. In order to test the nature of the kinetics a series of experiments was carried out with different partial pressures of each alcohol. All experiments were carried out at room temperature (297 K).

SiH_2 + MeOH

For the reaction with methanol the system was studied in three different ways. First (a) with no added buffer gas, then (b) with added SF_6 as buffer gas to a total pressure of 5 Torr, and finally (c) with SF_6 added at a fixed partial pressure of 2 Torr (but variable total pressure). The results of these experiments can be seen in Figure 1. Plots (a) and (c) are curved and show that the dependence of k_{obs} is not simply linear in [MeOH]. The data were fitted to the equation:

$$k_{obs} = k_{int} + k_1 x + k_2 x^2$$

Using LSQ fitting procedures rate constant values were obtained for each plot. These are shown in Table 1. The error limits are single standard deviations.

As we can see in Figure 1 this reaction system shows a significant total pressure dependence. This was investigated further using several buffer gases: Ar, N_2, C_3H_8 and SF_6. These experiments were done keeping the amount of MeOH fixed at 250 mTorr and varying the total amount of buffer gas. The second order rate constant was calculated using: k(second-order) = ($k_{obs} - k_{int}$)/[MeOH] at each of a set of total pressures up to 100 Torr. This is justified on the assumption that clean second order behaviour is shown at total pressures above 5 Torr, as indicated in Figure 1(b). The results are shown in Figure 2 in a log-log plot for convenience. It can be seen from the relative positions of the plots that Ar is the least efficient collider, followed by N_2 with C_3H_8 and SF_6 practically the same. Collision efficiencies were calculated by using RRKM modelling (see next section).

<u>SiH_2 + other alcohols</u>

For the remaining systems, viz SiH_2 with EtOH, 1-PrOH, 1-BuOH and 2-MBA experiments were done using different partial pressures of the alcohol but keeping the total pressure fixed at 10 Torr by addition of buffer gas (SF_6). Second order rate plots are shown in Figures 3 and 4 and we can see here that reasonably linear plots resulted. The second-order rate constants obtained by least-squares fitting are collected in Table 2. The error limits quoted are single standard deviations. It can be clearly seen that at 10 Torr total pressure the rate constants increase as the size of alcohol increases.

Just as with the MeOH, the pressure dependence of these reactions was also investigated, by carrying out experiments with small, but fixed, amounts of each alcohol and varying the total pressure using SF_6 as buffer gas. Second order kinetics was assumed. Figure 5 shows the pressure dependences of the rate constants for reactions of SiH_2 with the rest of

the alcohols studied in this work. As for SiH_2 with MeOH, the pressure dependences of the second order rate constants were fitted with RRKM models (see next section).

Ab initio calculations. Using the G3 method we examined first the energy surface for the $CSiH_6O$ species (SiH_2 + MeOH reaction). As expected, we found three stable species (or combination of species), viz (i) $H_2Si\cdots OHMe$, the initial complex of SiH_2 + MeOH, (ii) SiH_3OMe (methoxysilane), the lowest energy species on the surface, and (iii) H_2 + HSiOMe (methoxysilylene in both cis (c) and trans (t) forms). In addition we have located five transition states, TS1 leading from $H_2Si\cdots OHMe$ to SiH_3OMe, TS2c/TS2t leading from $H_2Si\cdots OHMe$ to H_2 + HSiOMe (c and t) via H_2 elimination and TS3c/TS3t connecting SiH_3OMe to H_2 + HSiOMe (c and t). The transition states for H_2 elimination from $H_2Si\cdots OHMe$ and from SiH_3OMe are clearly different from one another. The structures of all species are shown in Figure 6 and their enthalpy values are listed in Table 3 as well as being represented on the potential energy (enthalpy) surface in Figure 7.

We then turned our attention to the $C_2SiH_{10}O_2$ species (SiH_2 + 2MeOH reaction). Initially this was a more limited search designed to investigate the possible catalysed O-H insertion pathway of SiH_2 with methanol. Two new stable species were found, viz (i) $H_2Si\cdots(OHMe)_2$, a complex of SiH_2 with two molecules of methanol (which can also be regarded as an H-bonded complex of the second MeOH molecule with the initial $H_2Si\cdots OHMe$ complex) and (ii) $SiH_3O(Me)\cdots OHMe$, another H-bonded complex, in this case between methoxysilane and an MeOH molecule. The latter is the lowest energy species of these two and is essentially the reaction product. There is one transition state, TS4a, between (i) and (ii). It is worth noting that whereas TS1 (for SiH_2 + MeOH) lies above the reactants, TS4a (for SiH_2 + 2MeOH) lies well below the reactants in energy. The structures of these species are also shown in Figure 6 and enthalpies listed in Table 4. Because this exercise only allowed us to make an overall comparison of the catalytic effects of MeOH and H_2O[15], we

extended it to include the specific effects of MeOH and H_2O on the two zwitterions, $H_2Si{\cdot\cdot}OH_2$ and $H_2Si{\cdot\cdot}O(H)Me$ in order to try to gain greater insight. A summary of these results is also shown in Table 4 and further details are given in the supporting information.

As a final exercise we calculated the energies for forming the complexes between SiH_2 and the other alcohols which were studied experimentally in this work. These are shown in Table 5. The G3 procedure worked fine for all the reactions except that for SiH_2 with 2-MBA for which the molecular size was too large for the calculation. This system was calculated at the B3LYP/6-311+G(2d,p)//B3LYP/6-31G(d) level and then adjusted empirically by the amount (-15 kJ mol^{-1}) by which this level of calculation differed from G3 for the other four alcohols.

RRKM calculations. The pressure dependence of an association reaction corresponds exactly to that of the reverse unimolecular dissociation process providing there are no other perturbing reaction channels. Although the detailed ab initio calculations for SiH_2 + MeOH suggest the possibility of other channels there is no evidence from the kinetics (see discussion) of any such channel occurring under experimental conditions, and so we have carried out RRKM calculations[27] on the unimolecular dissociation processes of all the zwitterionic donor-acceptor complexes, $H_2Si{\cdots}OHR$, viz:

$$H_2Si{\cdots}OHR \rightarrow H_2Si + ROH \qquad (-1)$$

where R = Me-, Et-, 1-Pr-, 1-Bu- and $EtCHMeCH_2$-.

Since none of these complexes has been isolated, let alone studied experimentally, we are forced to make estimates of the necessary parameters for these calculations. This has been done as follows. First the likely Arrhenius *A* factors for these decomposition reactions were estimated. On the assumption of similar values for $\Delta S^o(1,-1)$ and log A_1 to those for $SiH_2 + H_2O$[18] and SiH_2 + cyclic ethers[28], values in the range 10^{15} to 10^{17} s^{-1} were initially investigated. These were now used to assign the vibrational wavenumbers for the transition state by adjustment of the key

transitional mode values of the zwitterionic species, using the standard Transistion State Theory formula, $A = (ekT/h)\exp(\Delta S^{\ddagger}/R)$. Since the wavenumbers for the reacting molecules (the zwitterions) were also not known they were estimated by use the known assignments for SiH_2[29] and MeOH[30] and the use of group values[31]. Whether precise values of all vibrational wavenumbers are correct or not is not important provided the entropies of activation, i.e. values of $\Delta S^{\ddagger}$, are matched. This applies also to models in which low wavenumber vibrations are replaced by internal rotations in the transition state[27]. An example of the assignment of both molecule and transition state, for decomposition of $H_2Si\cdots OHMe$, is shown in Table 6 which also includes the Lennard-Jones collision number value. The assignments for other choices of *A* factor and for the decompositions of the other zwitterionic species are shown in the supporting information. The values for the critical energies, E_o, employed in these calculations were those given by the ab initio calculations (Table 5). We have used a weak collisional (stepladder) model for collisional deactivation, because there is overwhelming evidence against the strong collision assumption[32]. The average energy removal parameter, $\langle\Delta E\rangle_{down}$ was taken as 12.0 kJ mol^{-1} (1000 cm^{-1}) when SF_6 was used as buffer gas (for all alcohols). For the other collider gases, used in the SiH_2 + MeOH studies, the values for $\langle\Delta E\rangle_{down}$ and Z_{LJ} are shown in Table 7.

The least well known feature of these calculations is the nature (tight or loose) of the transition states of these reactions. These determine both the positions of the "fall-off" curves and their curvatures. Thus optimising the fit to the experimental curves may be used to refine the transition state (characterised by its decomposition *A* factor) and also to pinpoint the value of k^{∞}, the high pressure limiting rate constant. This is illustrated for the SiH_2 + MeOH reaction in Figure 8. This shows the fits of the transition state models corresponding to values of 15 and 16 for log (A/s^{-1}). It can be seen that, although both models fit tolerably well, the latter provides the better fit. Using this model the pressure dependence data for the other buffer gases were fitted by

varying the collisional deactivation model step size. The fits are shown in Figures 9 and 10. Because one of the important modes of the decomposing molecule may be regarded as an internal rotation, we have further tested a model in which the lowest wavenumber vibration (the Si···O torsion) has been replaced by an internal rotation (in both molecule and transition state). This has been fitted to the looser transition state ($A = 10^{16}$ s^{-1}). The resulting fall-off curve is almost identical to that from the harmonic vibration only model, thus showing that this change makes little difference.

When the same exercise was carried out for the reactions of SiH_2 with the other alcohols, it was found necessary to extend the RRKM modelling to even looser transition states, up to those corresponding to $\log(A/s^{-1}) = 17$. The plots of best fit fall-off curves are shown in Figure 5. The summaries of the vibrational assignments for these models are given in the supporting information. The values of k^{∞} and the collisional efficiencies resulting from the fits, are given in Table 8. Again it was found that the substitution of an internal rotation for harmonic vibration in the molecular and transition state models made almost no difference to the fits. Other details, such as the Lennard Jones collision parameters, are also given in the supporting information.

As a separate exercise and in order to verify that the unimolecular conversion of the $H_2Si\cdots OHMe$ complex is not competitive under the conditions of these experiments, we constructed transition states for reaction via TS1 and TS2t. Details are given in the supporting information. Calculations were carried out at 297 K and the results are given in Table 9.

Discussion

General Comments and Rate Constant Comparisons. The main experimental purpose of this study was to measure the rate constants and their pressure dependences for the reactions of SiH_2 with alcohols. This has been accomplished. The only previous experimental information (in the gas phase) is for SiH_2 + MeOH[14]. Alexander, King and Lawrance (AKL)[14]

measured the rate constants at 294 K for SiH_2+ MeOH in Ar at total pressures of between 100 and 800 Torr. The only overlap with this work occurs at 100 Torr. The value found by AKL is 1.60×10^{-11} cm^3 molecule $^{-1}$ s^{-1} in reasonable agreement with our value of 1.80×10^{-11} cm^3 $molecule^{-1}s^{-1}$. A comparison of the experimental pressure dependence of the reaction in Ar observed by AKL with that from the RRKM modelling is, however, also possible (see below). There is no previous kinetic information for the reactions of SiH_2 with EtOH, 1-PrOH, 1-BuOH and 2-MBA with which to compare these results.

The present study of the reaction between SiH_2 and MeOH indicates a greater kinetic complexity than found hitherto. At pressures below 5 Torr, with or without added inert gas, the second order plots (Figure 1) show some curvature indicative of a rate component second order in MeOH, ie third order overall. The curvature is greatest in the experiments without added inert gas (Figure 1(a))[33]. In these experiments the total pressure is effectively that of MeOH and therefore any third body effect is changing from run to run. In the experiments at a total pressure of 5 Torr (Figure 1(b)) the bulk of the gas is comprised of SF_6 and the curvature is not apparent. The experiments carried out with 2 Torr of added SF_6 (Figure 1(c)) show only a slight curvature (just beyond the scatter of data points). Since in this set of experiments the pressure is varying less dramatically, this is some indication that MeOH might be exerting an effect other than that of a third body. Similar, but more clear-cut, effects were observed by us[15] in the SiH_2 + H_2O reaction. Although the effect found here is perhaps marginal, and the uncertainty high, it seemed nevertheless worthwhile to see whether the derived rate constant has a reasonable magnitude. The third order rate constant for the SiH_2 + MeOH reaction obtained here is compared with that for SiH_2 + H_2O in Table 10. Also included are those for the third body stabilisation process for SF_6 obtained from the RRKM modelling. Despite the uncertainties, the data show that the third order rate constants for SiH_2 + MeOH are both greater than those for SiH_2 + H_2O. This is to be expected since these numbers reflect the

stabilisation rate constants for the energised adducts ($H_2Si{\cdot\cdot}O(H)R^*$) which depend, in turn, on their densities of states which clearly increase with molecular size[27]. What is more striking is that for SF_6 as collision partner, the rate constant is an order of magnitude greater for the MeOH adduct compared with the H_2O adduct, whereas for MeOH compared with H_2O as collision partners, the rate constants increase by only ca a factor of two, although the uncertainty is particularly high. A different comparison of the numbers shows that the rate constant for stabilisation (or reaction) of the $H_2Si{\cdot\cdot}O(H)Me$ zwitterion by MeOH relative to SF_6 is 0.23 (± 0.19). Given that $Z_{LJ}(MeOH)/Z_{LJ}(SF_6)$ is 1.24 (see Table 7) the stabilising efficiency of MeOH compared with SF_6 is actually only 0.19 (± 0.16). This is the opposite of the relative efficiencies for SF_6 and H_2O (2.6 ± 0.2) in stabilising or reacting with $H_2Si{\cdot\cdot}OH_2$. While we cannot dismiss a catalysed process for MeOH, and its rate constant is comparable with (if not greater than) that for H_2O, the relativity with SF_6 is much less striking. For the reaction of SiH_2 with H_2O the high efficiency of the second H_2O molecule clearly pointed to a chemical effect. This was supported by the ab initio calculations which showed a low energy transition state corresponding to catalysed process (leading to SiH_3OH formation). While the kinetics evidence for a similar effect in the SiH_2 + MeOH reaction is much weaker, nevertheless it is supported by the ab initio calculations (see below and Figure 11). It should be pointed out that the quadratic effects observed here could not have been seen under the higher pressure conditions used by AKL[14].

Ab initio calculations and the mechanism. The calculations reported here are in reasonable accord with those of Heaven, Metha and Buntine (HMB)[13]. Table 3 compares our G3 enthalpy values with the ΔE(MP2) of HMB[13]. Although these are not identical quantities they are normally close to one another. Our enthalpy values for the zwitterion and TS1 are also in agreement with those of an earlier study by Lee and Boo[12] carried out at the MP4 level (not shown in the table). Compared with HMB[13] our study has identified an extra pathway to

the possible formation of H_2 + HSiOMe, viz via H_3SiOMe and TS3. Apart from this, the quantitative differences between the two studies are fairly small, the largest one being that of 18 – 20 kJ mol^{-1} between the values for TS2 (cis and trans) for formation of H_2 + HSiOMe directly from the zwitterion. Interestingly our values are negative (relative to SiH_2 + MeOH) whereas those of HMB[13] are positive. At first sight a negative value for either TS2c or TS2t might seem to suggest a facile reaction pathway for decay of the zwitterions but there is no indication of this from the experiments (see next section). However the structures of these transition states are tight corresponding to *A* factors in the range $10^{12} – 10^{13}$ s^{-1} (see supporting information) and so need to have more sizeable negative enthalpies for this pathway to be competitive with redissociation of the zwitterion to reactants (with its much looser transition state). The positive enthalpy for TS1, although not large in value, is sufficient, together with its also tight structure (and therefore low *A* factor), to explain why conversion of the zwitterion to stable product, methoxysilane is also ruled out. These arguments were verified as part of the RRKM calculations and the results discussed in the next section.

The calculations for reaction of SiH_2 with 2 molecules of MeOH show clearly that such a reaction is energetically feasible (both in terms of enthalpy and free energy). The transition state TS4a lies below the reaction threshold, showing that the $H_2Si\cdot\cdot(MeOH)_2$ complex can convert readily to the product H_3SiOMe(MeOH), ie the methoxysilane with a weakly complexed MeOH molecule. This is parallel to the reaction of SiH_2 with 2 molecules of H_2O, and a comparison of these two PE surfaces is shown in Figure 11. The diagram shows that the enthalpy surface for the MeOH case is more favourable than that of the H_2O case, since both the complex and its rearrangement transition state are lower in enthalpy relative to their respective reactants (by 28 and 31 kJ mol^{-1} respectively). Figure 11 also shows the further comparison with the PE surfaces for the catalysed reactions of SiH_2 + H_2O + MeOH, ie mixed catalysis (an exercise which is impossible to carry out experimentally). The data

calculated here (Table 4) allow us to obtain the following specific catalytic enthalpy values. Replacement of H_2O by MeOH in the zwitterionic position stabilises the complex by 21-22 kJ mol^{-1}, whereas replacement of H_2O by MeOH in the second (ie the catalytic) position stabilises the complex by only 6-7 kJ mol^{-1}. Since in the uncatalysed process, MeOH-for-H_2O substitution produces a zwitterionic stabilisation of 21 kJ mol^{-1}, this tells us that in the two molecule case, the substitution effect is only a modest 6 kJ mol^{-1} above the thermodynamic stabilisation of the zwitterion. The effect is slightly different on the transition state. MeOH-for-H_2O replacement in the zwitterionic position stabilises it by 17 kJ mol^{-1}, whereas in the catalytic position the stabilisation is 14 kJ mol^{-1}.The effects on the enthalpy barriers to the rearrangements of the two molecule complexes are more modest. The lowest barrier (30 kJ mol^{-1}) is for the H_2SiOH_2 zwitterion with MeOH catalysis and the highest (42 kJ mol^{-1}) is for the $H_2SiO(H)Me$ zwitterion with H_2O catalysis, but MeOH is clearly more effective as a catalyst. This undoubtedly arises because Me-for-H substitution facilitates the release of electron density which stabilises the transition state. Thus there is no doubt of the specific effect of MeOH relative to H_2O in producing a more favourable reaction enthalpy surface. However the further comparisons of entropy and free energy present a slightly more complex picture. Not surprisingly the entropy values for formation of the complexes and transition states are all highly negative. Differences amongst the four systems are not large, but it is clear that the transition state structures are all tighter than their respective complexes. The consequences of this are that transition state free energy values (for formation from respective reactant species) are very small and, in three cases, positive. Positive values, if small, are not a disqualification for reaction, nor an indication of a particularly slow reaction. This is clear since the most positive value is that for the $SiH_2 + H_2O$ reaction, the only gas-phase case for which the experimental evidence exists hitherto[15]. The only negative value is that for the reaction of $SiH_2 + 2MeOH$, studied here, which suggests it should, if anything, be more

favourable. Since the experimental evidence for catalysis is marginal, the rate constant for it (Table 10) represents an upper limit, which could be, within the uncertainties, either larger or smaller than that for SiH_2 + $2H_2O$. Thus we are forced to conclude that the balance of enthalpy and entropy effects combine to reduce any large difference between MeOH and H_2O on this intriguing catalytic process, and that the ab initio calculations have enough uncertainty within them not to give a clearcut answer.

RRKM calculations, their implications and the reaction efficiencies. All five reactions studied have been found to be pressure dependent and all five have been modelled. Only the reaction between SiH_2 and MeOH has been studied previously[14] and the only comparison possible, shown in Figure 12, is for the pressure dependence in Ar. While the rate constants of AKL[14] only overlap with ours at 100 Torr, the trends of the two data sets are closely similar and they also match reasonably well the RRKM calculated pressure dependence curve obtained here. AKL[14] also carried out RRKM calculations, using a Gorin model transition state which corresponded to log (A/s^{-1}) = 17.25. Their critical energy value (82 kJ mol^{-1}) was also slightly different from ours (74 kJ mol^{-1}, Table 4), although AKL chose to base their value on equilibrium measurements rather than their own ab initio value of 74.5 kJ mol^{-1}. We can only say that our own calculations support a model with a tighter transition state (at ambient temperatures) corresponding to log (A/s^{-1}) = 16.0 and that a model based on 17.25 would not fit the combined experimental data of Figure 12. The fits to pressure dependences for other bath gases (Figures 9 and 10) are all reasonably good which attests to the consistency of our model. The values found for $<\Delta E>_{down}$ are reasonably consistent with those expected for the bath gases used[32].

The lack of any obvious deviation to the pressure dependence curves at the lowest pressure (viz a levelling out) shows that no reactive exit channel for this reaction system can be competitive under the conditions. This enables us to put limits on the potential

unimolecular rearrangement channels, viz H_2 elimination from the $H_2Si{\cdot\cdot}O(H)Me$ zwitterion to form HSi-OMe and isomerisation to H_3SiOMe. The SiH_2 + MeOH + Ar system, produces the slowest rate constant at P = 5.1 Torr. The RRKM calculations give k = 0.6 s^{-1} for thermal redissociation of the zwitterions under these conditions. This provides the upper limit to the value for the rate constants for these rearrangement channels. In fact the limit should probably be an order of magnitude lower since the process is not visibly competitive. The value, nevertheless, shows that rearrangement is far too slow to be observed experimentally on the microsecond time frame of these experiments, even as a secondary process. The arguments against the occurrence of either of these processes are further supported by the results of the calculations of its rate constants based on the E_o values for TS1 and TS2t from the ab initio calculations. Table 9 shows that at the energies corresponding to the maximum populations of energized zwitterion species (E_o + thermal energy) the rate of the redissociation process exceeds that of unimolecular rearrangement by factors in excess of 100 for H_2 elimination and 1000 for isomerisation.

For the reactions of SiH_2 with the other alcohols, the fits of the RRKM calculated pressure dependences to the experimental results (Figure 5) are reasonably good. The fits for 1-propanol and 1-butanol are very close but apparently cross; we suspect that this is an artefact arising from experimental error. Of course the models are matched to the curvature of these pressure dependences and so the fits have been optimised. The judgement of their success depends to a large extent on whether they produce reasonable values for the high pressure limiting rate constants, k^{∞}. The values derived (at 297 K), shown in Table 8, are all very close to the Lennard-Jones collision limits, corresponding to ca 60% of the value if the best fit models are used. Even with the less good fitting models the efficiencies are still quite high. Although for SiH_2 + EtOH the values of k^{∞} and the efficiency look slightly low, they are within the uncertainties of the values for the other systems. The rate constants increase with

molecular mass and size of the alcohol, as expected, and the pressure dependences get less. The consequence of this is that, extrapolation to k^{∞} can be done with more confidence and less reliance on the RRKM model. Thus we can be reasonably confident in the values for these high efficiencies, particularly for the larger alcohols. It should be noted that the RRKM model used by AKL[10] for SiH_2 + MeOH gives a value for k^{∞} of 1.43×10^{-9} cm^3 $molecule^{-1}$ s^{-1}, a factor of ca 4.5 times greater than our extrapolated value corresponding to an efficiency of ca 290%. Although AKL[14] have explained this in terms of long range interactions, leading to an unusually high collision cross section, our results show that such an explanation is not necessary.

Conclusions

The findings of this work support the view that the reaction of silylene with an alcohol is a simple association process leading to a zwitterionic, donor-acceptor complex as the final product in the gas phase. The measured second-order rate constants for reactions of SiH_2 with five alcohols are pressure dependent and, when extrapolated to infinite pressure by the use of RRKM theory, show that the reactions are occurring at close to the Lennard-Jones collision rate. The use of larger alcohols reduces significantly the extent of extrapolation necessary, and improves the reliability of this conclusion compared with that from the modelling of data for SiH_2 + MeOH alone. For the latter reaction, the finding of a kinetic component second order in MeOH, suggests the existence of an additional catalysed reaction pathway. This is supported by ab initio calculations, which indicate a low energy process whereby the complex reacts with a second molecule of MeOH which converts it into methoxysilane (+ MeOH). The energetics of this process have been explored with other similar model processes, which define some specific MeOH-for-H_2O substitution effects. This catalytic pathway, although at the limit of our detection capability, is nevertheless consistent with the solution findings of

Leigh's group[8] for the process of conversion of zwitterionic complexes into silyl ethers (siloxanes) in solution.

Acknowledgement. R.B. thanks the Ministerio de Educacion y Ciencia for support under Project CTQ2006-10512 and Royal Society of Chemistry for a journals grant.

Supporting Information Available: Details of vibrational assignments for the SiH_2··ROH complexes and their decomposition transition states and Lennard-Jones parameters for molecules of interest. This material is available free of charge via the Internet at http://pubs.acs.org.

References and Notes

(1) Gaspar, P. P.; West, R. Silylenes. In *The Chemistry of Organic Silicon Compounds*; Rappoport, Z., Apeloig, Y., Eds.; Wiley: Chichester, 1998; Vol. 2, Chapter 43, p 2463.

(2) Jasinski, J. M.; Becerra, R.; Walsh, R. *Chem. Rev.* **1995**, *95*, 1203.

(3) Becerra, R.; Walsh, R. Kinetics & mechanisms of silylene reactions: A prototype for gas-phase acid/base chemistry. In *Research in Chemical Kinetics*; Compton, R. G., Hancock, G., Eds.; Elsevier: Amsterdam, 1995; Vol. 3, p 263.

(4) Becerra, R.; Walsh, R. *Phys. Chem. Chem. Phys.* **2007**, *9*, 2817.

(5) Gillette, G. R.; Noren, G. H.; West, R. *Organometallics* **1989**, *8*, 487.

(6) Levin, G.; Das, P. K.; Bilgrien, C.; Lee, C. L. *Organometallics* **1989**, *8*, 1206.

(7) Moiseev, A. G.; Leigh, W. J. *Organometallics* **2007**, *26*, 6277.

(8) Leigh, W. J.; Kostina, S. S.; Bhattacharya, A.; Moiseev, A. G. *Organometallics* **2010**, *29*, 662.

(9) Tokitoh, N.; Ando, W. In *Reactive Intermediate Chemistry*, Moss, R. A., Platz, M. S., Jones, M. Jr., Eds.; Wiley & Sons, NY, 2004, Chapter 14, p. 651

(10) Raghavachari, K.; Chandrasekhar, J.; Gordon, M. S.; Dykema, K. J. *J. Am. Chem. Soc.* **1984**, *106*, 5853.

(11) Su, S.; Gordon, M. S. *Chem. Phys. Lett.* **1993**, *204*, 306.

(12) Lee, S. Y.; Boo, B. H. *J. Mol. Struct. (THEOCHEM)* **1996**, *366*, 79.

(13) Heaven, M. W.; Metha, G. F.; Buntine, M. A. *J. Phys. Chem. A* **2001**, *105*, 1185.

(14) Alexander, U. N.; King, K. D.; Lawrance, W. D. *J. Phys. Chem. A* **2002**, *106*, 973.

(15) Becerra, R.; Goldberg, N.; Cannady, J. P.; Almond, M. J.; Ogden, J. S.; Walsh, R. *J. Am. Chem. Soc*. **2004**, *126*, 6816.

(16) Baggott, J. E.; Blitz, M. A.; Frey, H. M.; Lightfoot, P. D.; Walsh, R. *Int. J. Chem. Kinet.* **1992**, *24*, 127.

(17) Alexander, U. N.; King, K. D.; Lawrance, W. D. *Phys. Chem. Chem. Phys.* **2001**, *3*, 3085.

(18) Becerra, R.; Cannady, J. P.; Walsh, R. *J. Phys. Chem. A* **2003**, *107*, 11049.

(19) Steele, K. P.; Weber, W. P. *Inorg Chem.* **1981**, *20*, 1302.

(20) Steele, K. P.; Tseng, D.; Weber, W. P. *J. Organometal. Chem*. **1982**, *231*, 291.

(21) Becerra, R.; Carpenter, I. W.; Gutsche, G. J.; King, K. D.; Lawrance W. D.; Staker, W. S.; Walsh, R. *Chem. Phys. Lett.* **2001**, *333*, 83.

(22) Jasinski, J. M.; Chu, J. O. *J. Chem. Phys.* **1988**, *88*, 1678.

(23) Damrauer, R.; Simon, R.; Laporterie, A.; Manuel, G.; Tae Park, Y.; Weber, W. P. *J. Organomet. Chem.* **1990**, *391*, 7.

(24) Frisch, M. J.; Trucks, G. W.; Schlegel, H. B.; Scuseria, G. E.; Robb, M. A.; Cheeseman, J. R.; Montgomery, Jr., J. A.; Vreven, T.; Kudin, K. N.; Burant, J. C.; Millam, J. M.; Iyengar, S. S.; Tomasi, J.; Barone, V.; Mennucci, B.; Cossi, M.; Scalmani, G.; Rega, N.; Petersson, G. A.; Nakatsuji, H.; Hada, M.; Ehara, M.; Toyota, K.; Fukuda, R.; Hasegawa, J.; Ishida, M.; Nakajima, T.; Honda, Y.; Kitao, O.; Nakai, H.; Klene, M.; Li, X.; Knox J. E.; Hratchian,H. P.; Cross,J. B.; Bakken, V.; Adamo, C.; Jaramillo, J.; Gomperts, R.;

Stratmann, R. E.; Yazyev, O.; Austin, A. J.; Cammi, R.; Pomelli, C.; Ochterski, J. W.; Ayala, P. Y.; Morokuma, K.; Voth, G. A.; Salvador, P.; Dannemberg, J. J.; Zakrzewski, V. G.; Dapprich, S.; Daniels, A. D.; Strain, M. C.; Farkas, O.; Malick, D. K.; Rabuck, A. D.; Raghavachari, K.; Foresman, J. B.; Ortiz, J. V.; Cui, Q.; Baboul, A. G.; Clifford, S.; Cioslowski, J.; Stefanov, B. B.; Liu, G.; Liashenko, A.; Piskorz, P.; Komaromi, R.; Martin, R. L.; Fox, D. J.; Keith, T.; Al-Laham, M. A.; Peng, C. Y.; Nanayakkara, A.; Challacombe, M.; Gill, P. M. W.; Johnson, B.; Chen, W.; Wong, M. W.; Gonzales, C. and Pople, J. A., *Gaussian 03*, revision E.01, Gaussian, Inc., Wallingford CT, 2004

(25) Curtiss, L. A.; Raghavachari, K.; Redfern, P. C.; Rassolov, V.; Pople, J. A. *J. Chem. Phys.* **1998**, *109*, 7764.

(26) Gonzales, C.; Schlegel, H. B. *J. Chem. Phys.* **1989**, *90*, 2154.

(27) Holbrook, K.A.; Pilling, M.J.; Robertson, S.H. *Unimolecular Reactions*, 2nd ed.; Wiley: Chichester, 1996.

(28) Becerra, R.; Cannady, J. P.; Goulder, O.; Walsh, R. *J. Phys. Chem. A* **2010**, *114*, 784

(29) Fredin, L.; Hange, R. H.; Kafafi, Z. H.; Margrave, J. L. *J. Phys. Chem*. **1985**, *82*, 3542.

(30) Shimamouchi, T. *Molecular vibration frequencies*. Tables of Molecular vibration frequencies, Consolidated Volume 1, NRDS-NB539, 1972.

(31) Benson, S. W. *Thermochemical Kinetics*, 2nd ed.; Wiley: New York, 1976.

(32) Hippler, H.; Troe, J. in *Advances in Gas Phase Photochemistry and Kinetics*, Ashfold, M. N. R.; Baggott, J. E., Eds.; Royal Society of Chemistry: London, 1989, Vol. 2, Chapter 5, p. 209.

(33) A referee has queried whether this could be due to diffusion. We calculate that for 10% of SiH_2 to be lost in this way from the observation zone at 1 Torr MeOH, a diffusion rate constant of ca 10^3 s^{-1} would be required, based on a estimated value of 83 cm^2 s^{-1} for the

diffusion constant (see supporting information). This value is an order of magnitude too low to account for the observed decay signals.

TABLE 1: Rate constants from second order plots (including quadratic fitting) for SiH_2 + MeOH at 297 K

Total Pressure[a]	k_{int}/s^{-1}	k_1[b]	k_2[c]
(a) variable	4.1 ± 1.1	2.6 ± 0.9	2.9 ± 1.2
(c) variable	4.6 ± 0.6	4.5 ± 0.6	1.3 ± 1.1
(b) 5 Torr	4.66 ± 0.45	5.85 ± 0.13	–

[a] see text for conditions [b]Units: 10^{-12} cm^3 $molecule^{-1}$ s^{-1}
[c]Units: 10^{-29} cm^6 $molecule^{-2}$ s^{-1}

TABLE 2: Experimental second-order rate constants for SiH_2 + ROH at 10 Torr total pressure and 297 K

ROH	k/ cm^3 $molecule^{-1}$ s^{-1}
MeOH[a]	$(5.85 \pm 0.13) \times 10^{-12}$
EtOH	$(3.44 \pm 0.24) \times 10^{-11}$
1-PrOH	$(8.52 \pm 0.37) \times 10^{-11}$
1-BuOH	$(1.07 \pm 0.05) \times 10^{-10}$
2-MBA[b]	$(1.65 \pm 0.07) \times 10^{-10}$

[a] at 5 Torr total pressure [b]2-methyl-1-butanol

TABLE 3: Ab initio G3 Enthalpies for Species of Interest in the SiH_2 + MeOH Reaction

Molecular Species	G3 Enthalpy[a]	Relative[b]	HMB[b,c]
	$CSiH_6O$		
SiH_2 + MeOH	-406.078635	0	0
$H_2Si\cdots OHMe$	-406.107957	-77	-75.8
TS1	-406.077746	+2	+12.5
H_3SiOMe	-406.197471	-312	-304.1
TS2c	-406.079696	-3	+16.1
TS2t	-406.080087	-4	+14.9
H_2 + HSiOMe(c)	-406.132165	-138	-128.1
H_2 + HSiOMe(t)	-406.131030	-140	-125.5
TS3c	-406.098289	-52	-
TS3t	-406.094839	-43	-

[a] H^o (298K) values in Hartrees. [b] Relative energy in kJ mol^{-1}
[c] MP2/6-311++G(d,p) level, ref 13.

TABLE 4: Ab initio G3 Thermodynamic Quantities at 298 K for Species of Interest in the SiH_2 + 2MeOH and related Reactions

Molecular Species	$\Delta H^{a,b}$	$\Delta S^{a,c}$	$\Delta G^{a,b}$
SiH_2 + 2MeOH	0	0	0
$H_2Si\cdots(OHMe)_2$	-129	-267	-49
TS4a	-95	-311	-2
$H_3SiO(Me)\cdots HOMe$	-331	-254	-255
$H_3SiO(Me)$ + MeOH	-312	-149	-268
SiH_2 + $2H_2O$	0	0	0
$H_2Si\cdots(OH_2)_2$	-101(-103[b])	-248	-27
TS4b	-64(-59[b])	-291	+23
$H_3SiO(H)\cdots HOH$	-317(-317[b])	-239	-246
H_3SiOH + H_2O	-305(-305[b])	-139	-264
SiH_2 + H_2O + MeOH	0	0	0
$H_2Si\cdots OH_2\cdots OHMe$	-108	-254	-32
TS4c	-78	-298	+11
$H_3SiO(H)\cdots HOMe$	-320	-237	-249
H_3SiOH + MeOH	-305	-139	-264
SiH_2 + MeOH + H_2O	0	0	0
$H_2Si\cdots OHMe\cdots OH_2$	-123	-262	-45
TS4d	-81	-301	+9
$H_3SiO(Me)\cdots$ HOH	-326	-247	-252
H_3SiOMe + H_2O	-312	-149	-268

[a]Values relative those of reactant species [b]Units: kJ mol^{-1} [c]Units J K^{-1} mol^{-1}

[d]Ref. 15

TABLE 5: Ab initio G3 calculated energies of formation (kJ mol^{-1}) of silylene complexes of ROH

ROH	ΔE (0 K)	ΔH (298 K)[a]	ΔG (298 K)
MeOH	-73.54	-77 (-62)	-36.0
EtOH	-77.69[b]	-80 (-64)	-39.6
1-PrOH	-78.32	-81 (-65)	-40.1
1-BuOH	-78.96	-82 (-65)	-40.6
2-MBA	-76.50	-77[c]	-

[a] Values in parenthesis at B3LYP level. [b]*cf* -78.6 at MP2/6-311++G(d,p) level, ref 13.

[c]Approx value (see text)

TABLE 6: **Molecular and Transition State Parameters for RRKM Calculations for Decomposition of the $H_2Si\cdots OHCH_3$ Adduct**

Parameter	Molecule	TS(297K)
C-H str(3)	3000, 2960, 2844	3000, 2960, 2844
O-H str	3663	3663
Si-H str(2)	1965, 1918	1965, 1918
C-O str	1033	1033
CH_3 def (3)	1477(2), 1455	1477(2), 1455
CH_3 rock (2)	1165, 1060	1165, 1060
CÔH bend	1355	1355
SiH_2 bend	977	977
Si-O str	776	rxn coord
SiÔC bend	200	50
HÔSi bend	500	60
SiH_2 wag	651	105
SiH_2 rock	257	90
C-O torsion	250	250
Si···O torsion	150	70
A/s^{-1}		1.0×10^{16}
E_o/kJ mol^{-1}		73.54
$Z_{LJ}/10^{-10}$ cm^3 molec^{-1} s^{-1}		4.94

TABLE 7: Lennard-Jones Collision numbers and energy removal parameters for collider gases

Parameter	Ar	N_2	C_3H_8	SF_6	MeOH
$Z_{LJ}/10^{-10}$ cm^3 molec^{-1} s^{-1}	4.035	5.983	6.497	4.94	6.11
$\langle \Delta E \rangle_{down}$/ cm^{-1}	450	400	650	1000	-

TABLE 8: Summary of high pressure limiting rate constants for reactions of SiH_2 with alcohols from best fit RRKM calculations, together with collision efficiency estimates

Parameter	MeOH	EtOH	1-PrOH	1-BuOH	2-MBA
$\log(k^{\infty}/\ cm^3\ molecule^{-1}\ s^{-1})$	-9.5[a](-10.1)[b]	-9.72[a]	-9.45[c](-9.62)[a]	-9.4[d](-9.80)[a]	-9.35[d](-9.63)[a]
$k^{\infty}/10^{-10} cm^3\ molecule^{-1}\ s^{-1}$	3.16[a](0.79)[b]	2.00[a]	3.55[c](2.40)[a]	3.98[d](1.58)[a]	4.47[d](2.34)[a]
$Z_{LJ}/10^{-10} cm^3\ molecule^{-1}\ s^{-1}$	5.12	5.305	5.973	5.946	6.525
% Efficiency	62(15)	38	59(40)	67(27)	69(36)

[a] $\log(A/s^{-1}) = 16.0$ [b] $\log(A/s^{-1}) = 15.0$ [c] $\log(A/s^{-1}) = 16.5$ [d] $\log(A/s^{-1}) = 17.0$

TABLE 9: Comparison of energy specific rate constants, $k_1(E^*)$, for potential unimolecular rearrangement pathways of the $H_2Si{\cdot\cdot}OMe$ zwitterions calculated via RRKM theory using the ab initio potential energy surface

E^*/cm^{-1} [a]	$k_{diss}(E^*)/s^{-1}$ [b]	$k_1(E^*)/s^{-1}$ [c]	k_1/k_{diss}	$k_{2t}(E^*)/s^{-1}$ [d]	k_{2t}/k_{diss}
6600	1.36×10^9	0	-	1.73×10^7	1.3×10^{-2}
6800	4.60×10^9	2.25×10^6	4.9×10^{-4}	3.16×10^7	6.8×10^{-3}
7000[e]	1.16×10^{10}	7.04×10^6	6.1×10^{-4}	5.28×10^7	4.6×10^{-3}
7200	2.40×10^{10}	1.24×10^7	5.2×10^{-4}	7.18×10^7	3.0×10^{-3}
7400	4.36×10^{10}	1.74×10^7	4.0×10^{-4}	1.02×10^8	2.3×10^{-3}

[a] 1 cm^{-1} = 11.96 J mol^{-1} [b] k for dissociation [c] k via TS1 [d] k via TS2t [e] Energy of maximum population of energized molecules

TABLE 10: Third-order (limiting) rate constants for reactions of SiH_2 with H_2O and MeOH at 297 K for ROH (H_2O or MeOH) and SF_6 as third bodies

Reaction	$k/10^{-29}\ cm^3\ molecule^{-1}\ s^{-1}$	
	+ROH[c,d]	+SF_6
$SiH_2 + H_2O$[a]	0.60 ± 0.04[c]	0.23
SiH_2 + MeOH[b]	1.3 ± 1.1[d]	5.60

[a] Ref 15. [b] This work [c] ROH = H_2O [d] ROH = MeOH

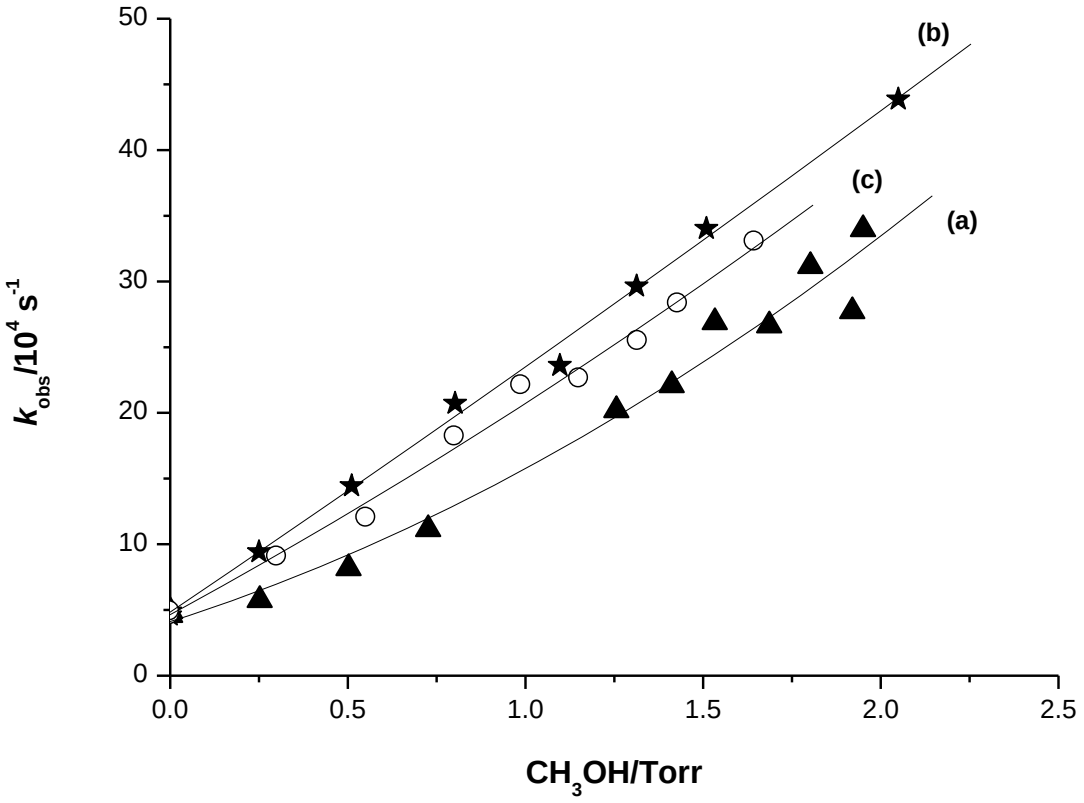

Figure 1. Second order rate plots for the reaction of SiH_2 + MeOH at 297 K under various conditions: ▲, no buffer gas; ★, 5 Torr total pressure (made up with SF_6); ○, 2 Torr added SF_6. Lines are LSQ best fits: (a) and (c) quadratic; (b) linear.

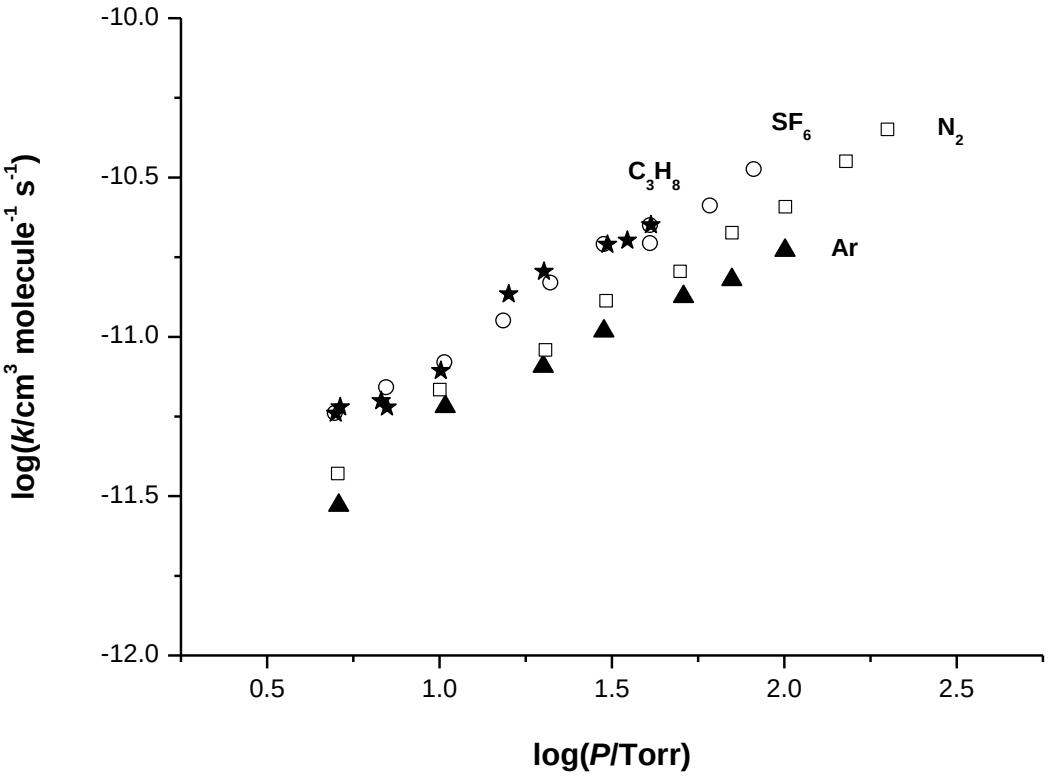

Figure 2. Pressure dependence of the second order rate constants for SiH_2 + MeOH at 297 K with different colliders, as indicated.

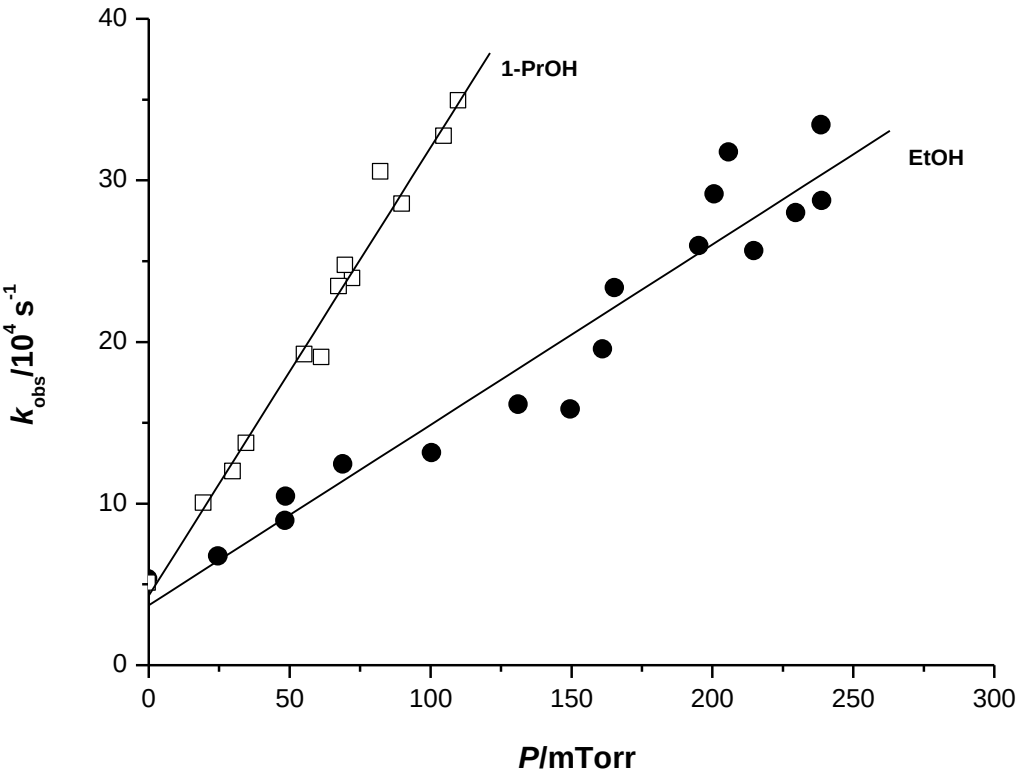

Figure 3. Second order plot for the reactions of SiH_2 with EtOH and 1-PrOH at a total pressure of 10 Torr (added SF_6) at 297 K.

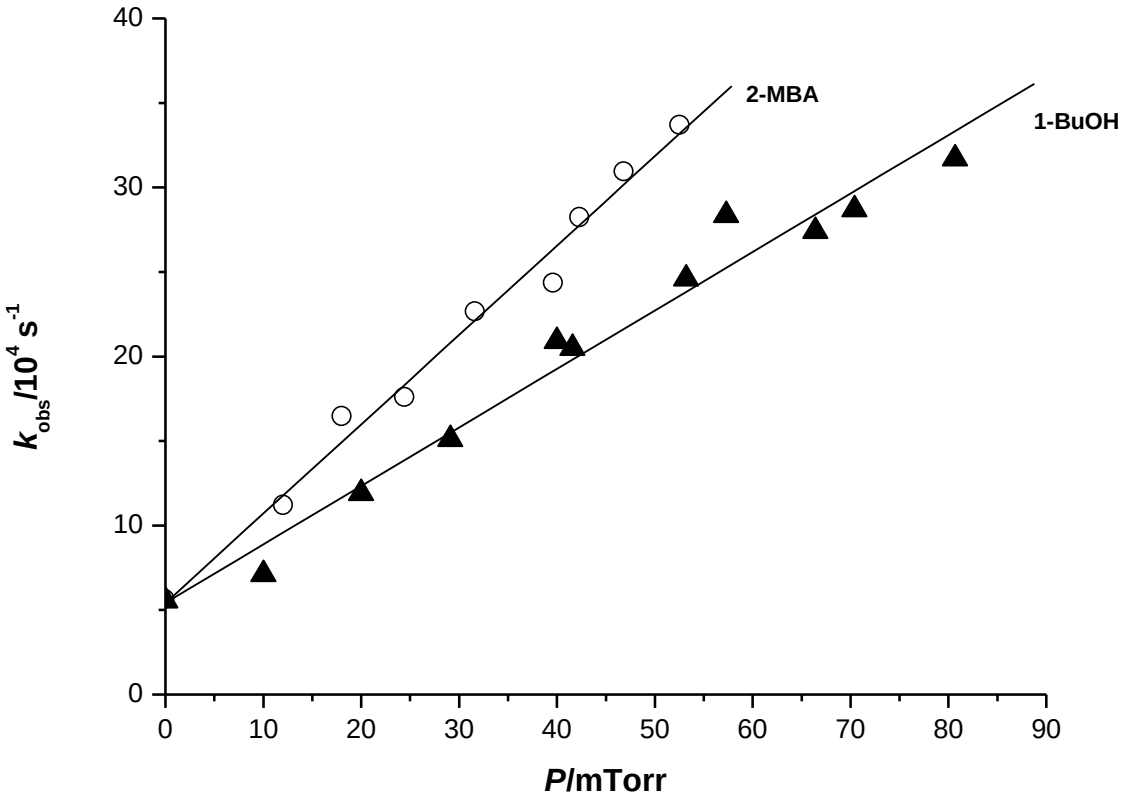

Figure 4. Second order plot for the reactions of SiH_2 with 1-BuOH and 2-MBA at 10 Torr total pressure (added SF_6) at 297 K.

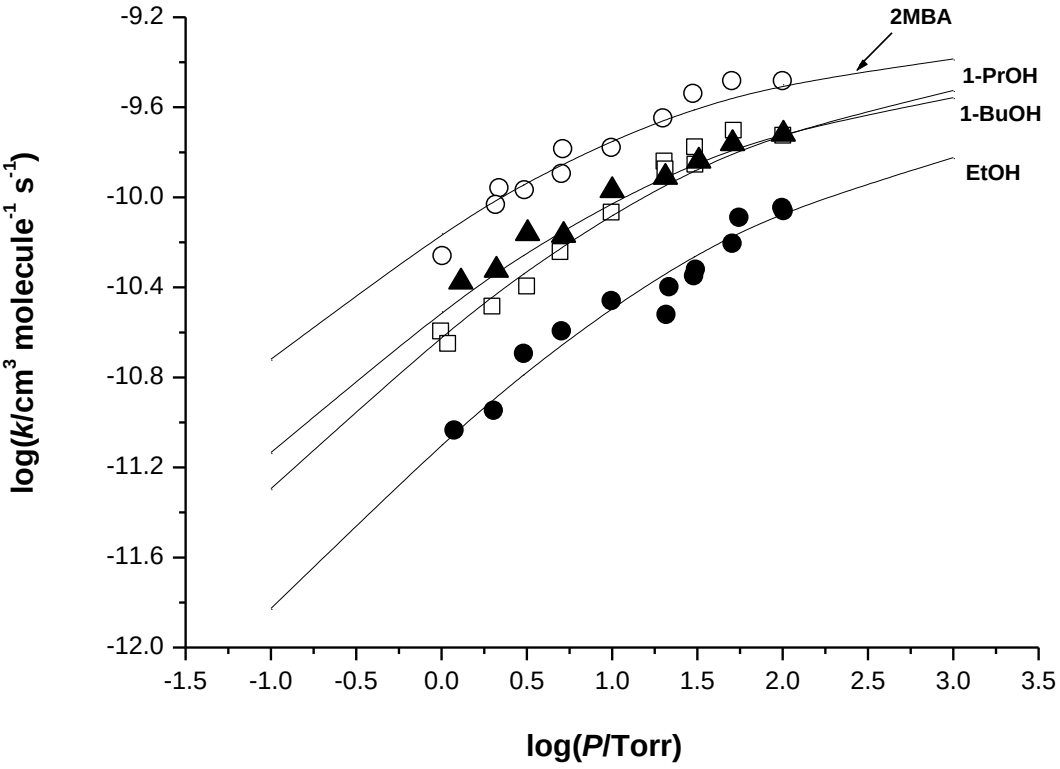

Figure 5. Pressure dependences for the second order rate constants for SiH_2 + ROH: ●, EtOH; □, 1-PrOH; ▲, 1-BuOH; ○, 2-MBA. Lines are RRKM theory best fits (see text).

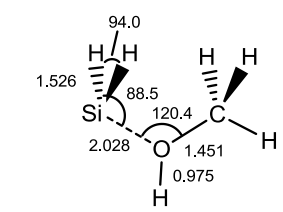

$H_2Si\cdots OHMe$

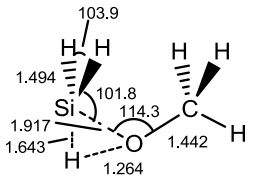

TS1

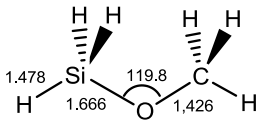

H_3SiOMe

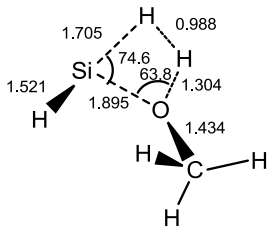

TS2c

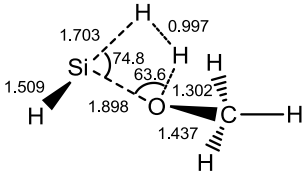

TS2t

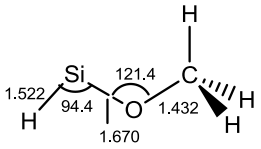

HSiOMe(t)

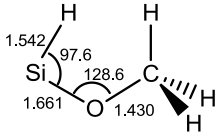

HSiOMe(c)

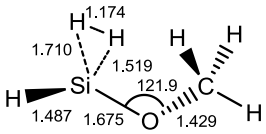

TS3t

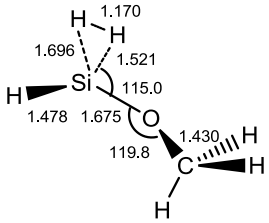

TS3c

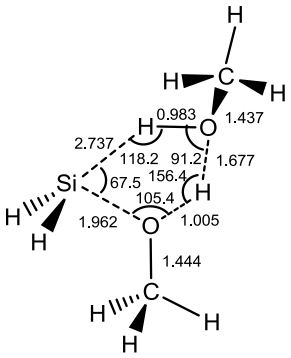

$H_2Si\cdot(OHMe)_2$

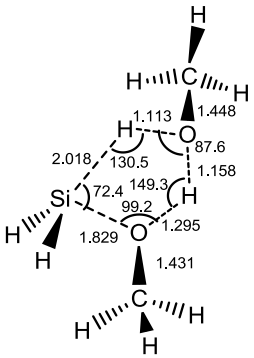

TS4a

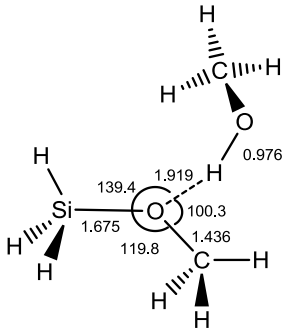

$H_3SiO(Me)\cdots HOMe$

Figure 6. Ab initio calculated (G3 level) geometries of local minima and transition states on the energy surfaces of the SiH_2 + MeOH and SiH_2 + 2MeOH reactions. Selected distances are given in Å, and angles are in degrees.

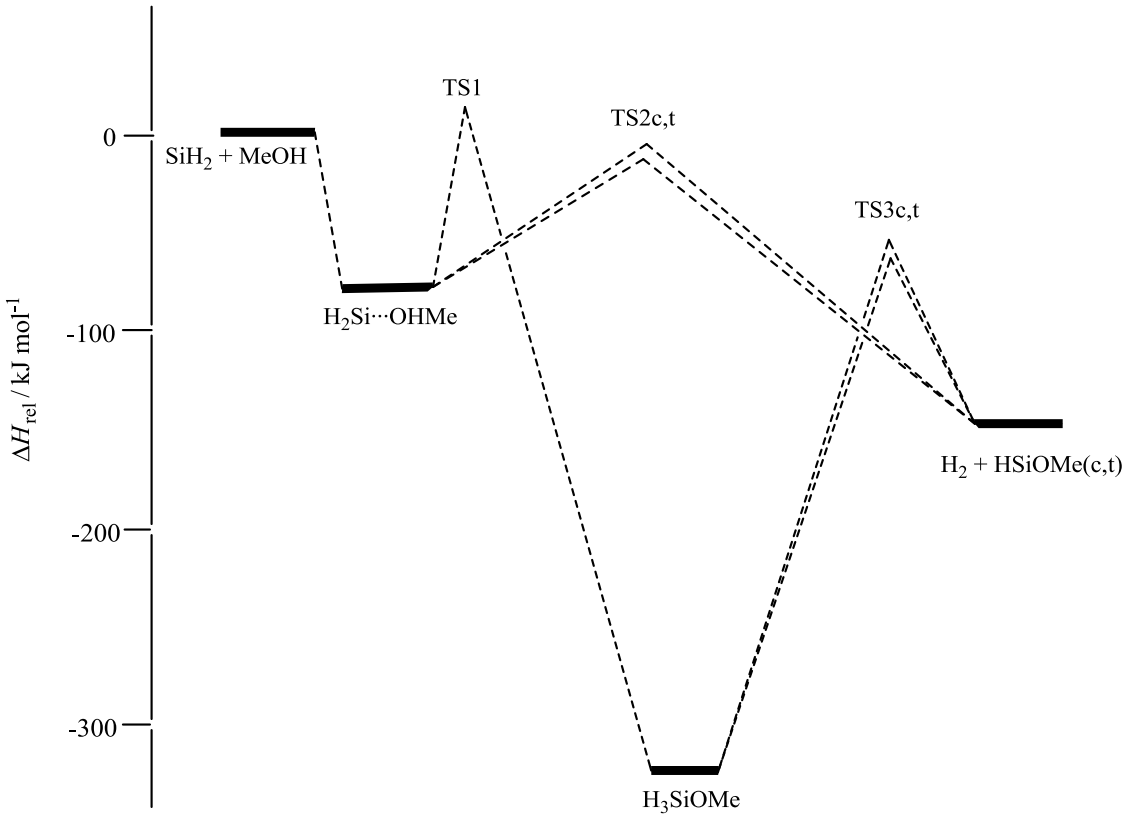

Figure 7. Potential energy (enthalpy) surface for the reaction of SiH_2 + MeOH. All enthalpies are calculated at the G3 level.

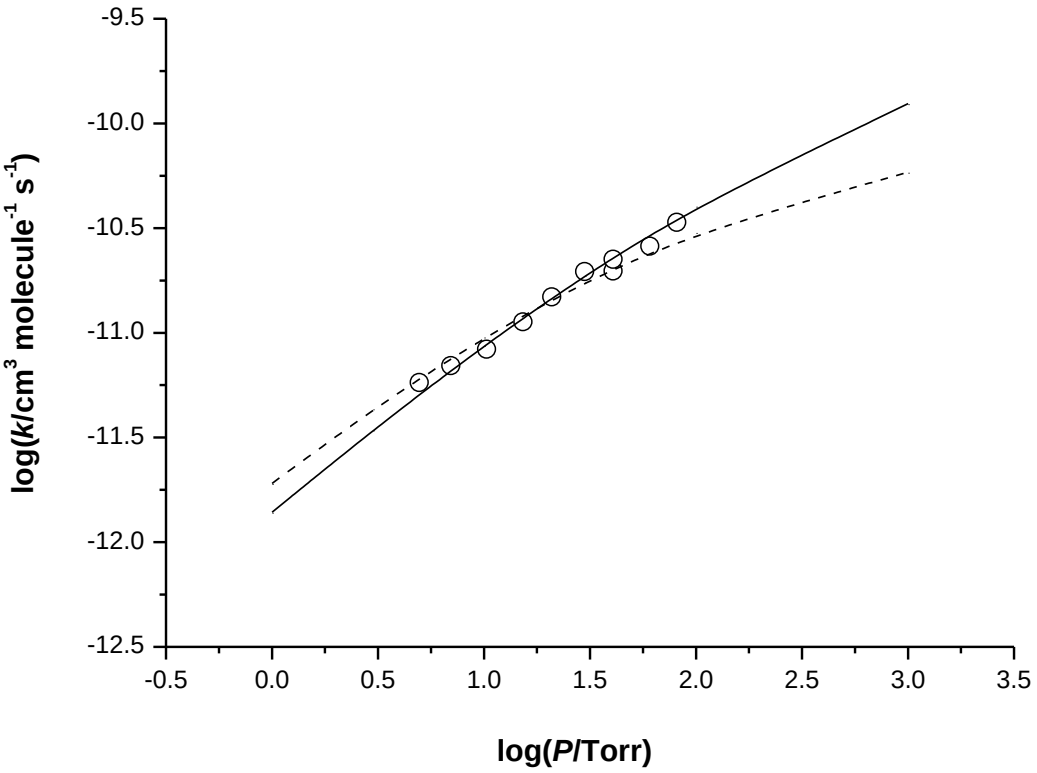

Figure 8. RRKM model fits to the pressure dependence for SiH_2 + MeOH (in SF_6). Models: —, log (A/s^{-1}) = 16.0; ----, log (A/s^{-1}) = 15.0)

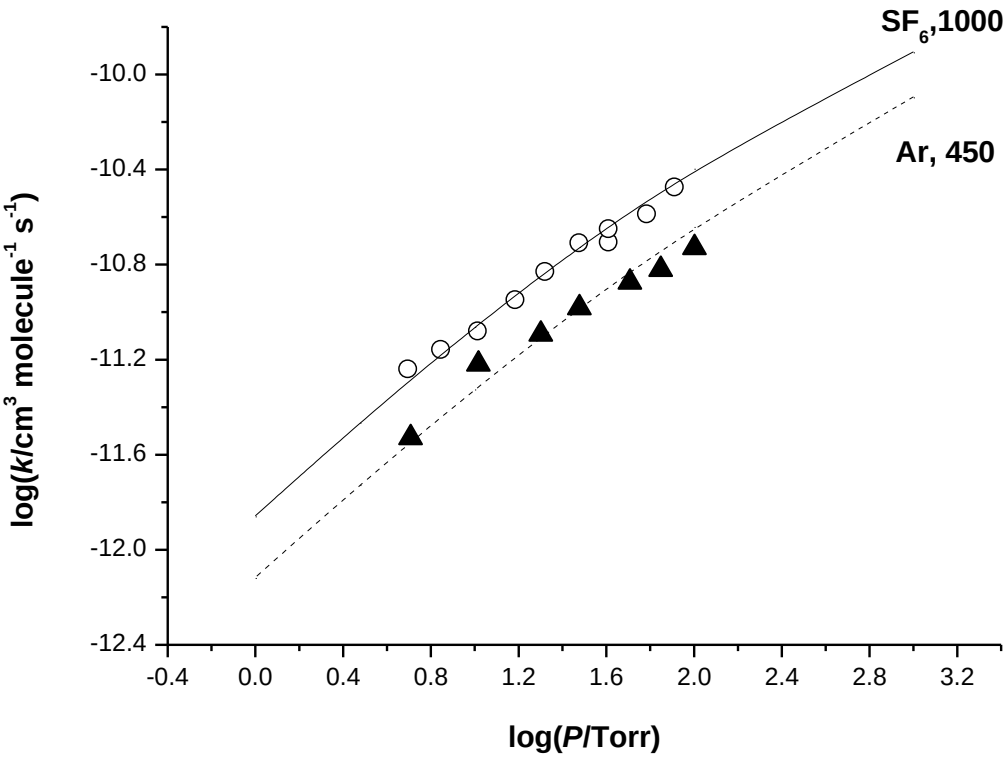

Figure 9. RRKM model (log (A/s^{-1}) = 16.0) fits to the pressure dependence for SiH_2 + MeOH. Data points: ○, SF_6; ▲, Ar. Lines and step sizes indicated.

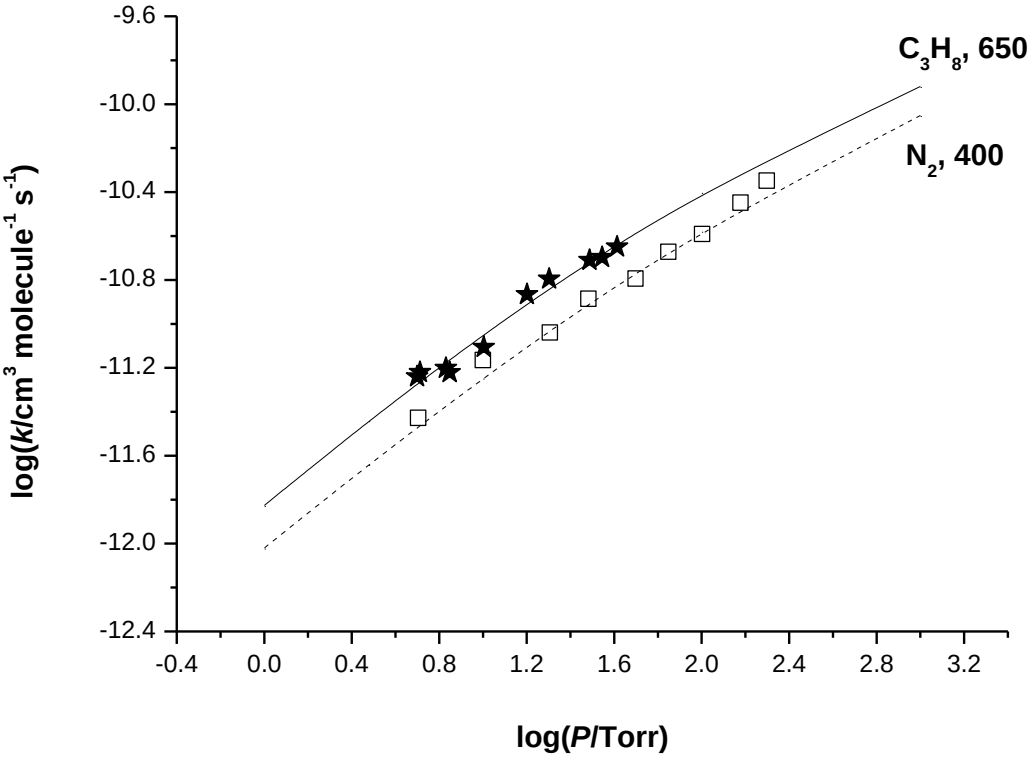

Figure 10. RRKM model (log (A/s^{-1}) = 16.0) fits to the pressure dependence for SiH_2 + MeOH. Data points: ★, C_3H_8; □, N_2. Lines and step sizes indicated.

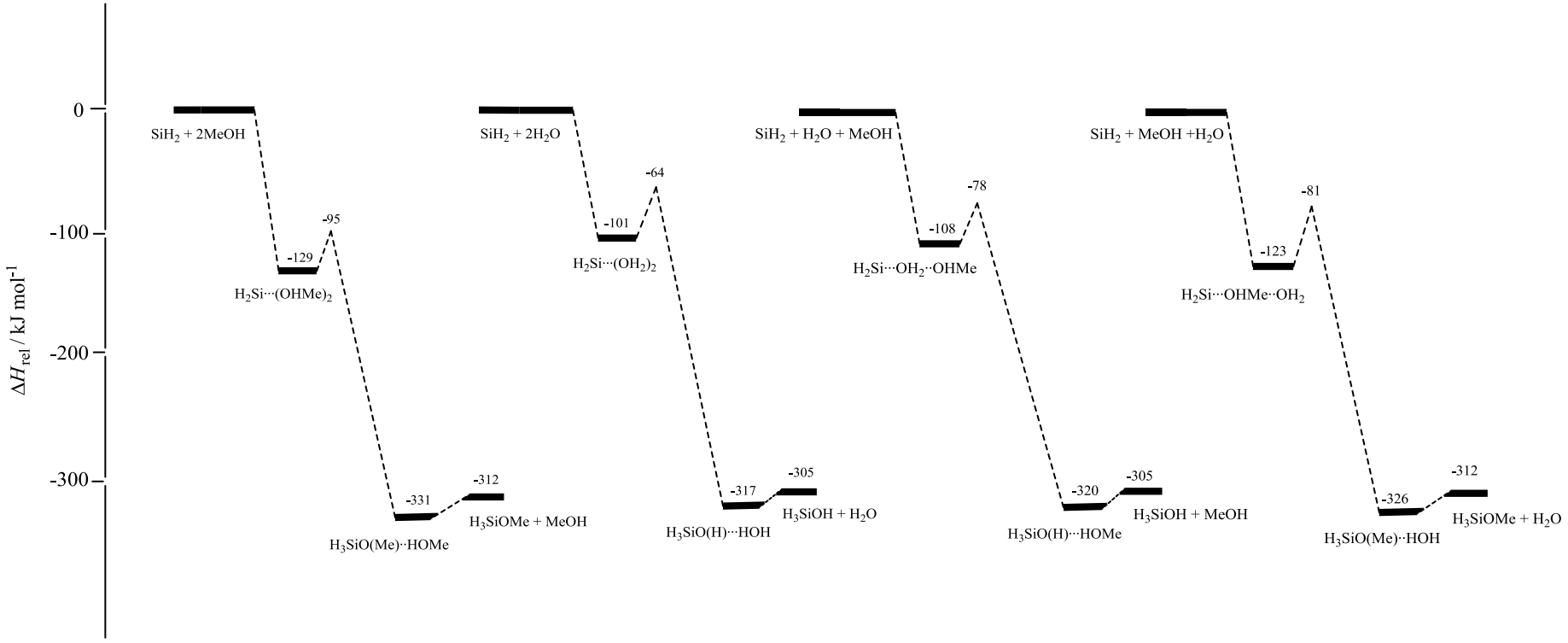

Figure 11. Comparison of PE surface (G3 level) for SiH_2 + 2MeOH with those for SiH_2 + $2H_2O$ and SiH_2 + MeOH + H_2O.

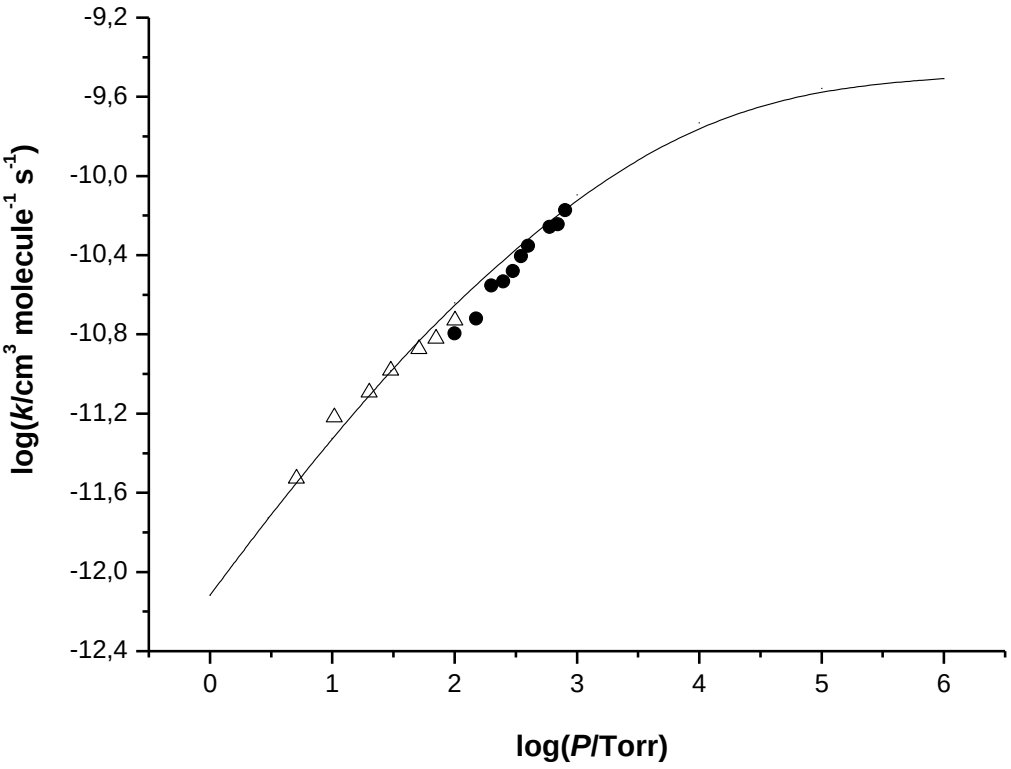

Figure 12. RRKM model (log (A/s^{-1}) = 16.0) fit to the pressure dependence for SiH_2 + MeOH (in Ar). Experimental data: △, this work; ●, reference 14.